**Article:**

Kamkeng, A.D.N. and Wang, M. orcid.org/0000-0001-9752-270X (2023) Technical analysis of the modified Fischer-Tropsch synthesis process for direct CO2 conversion into gasoline fuel: performance improvement via ex-situ water removal. Chemical Engineering Journal, 462. 142048. ISSN 1385-8947

https://doi.org/10.1016/j.cej.2023.142048

Chemical Engineering Journal 462 (2023) 142048

Contents lists available at ScienceDirect

Chemical Engineering Journal

journal homepage: www.elsevier.com/locate/cej

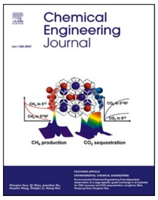

# Technical analysis of the modified Fischer-Tropsch synthesis process for direct $CO_2$ conversion into gasoline fuel: Performance improvement via ex-situ water removal

Ariane D.N. Kamkeng, Meihong Wang *

*Department of Chemical and Biological Engineering, University of Sheffield, Mappin Street, Sheffield S1 3JD, United Kingdom*

A R T I C L E   I N F O

*Keywords:*
$CO_2$ utilisation
Modified Fischer-Tropsch synthesis
Gasoline
Water removal
Modelling and simulation

A B S T R A C T

The modified Fischer-Tropsch synthesis (FTS) process is a promising technology for direct $CO_2$ conversion into liquid fuels. However, the low yield of liquid fuels (below 29%) observed during $CO_2$-FTS process is still of great concern for commercial deployment. Therefore, new strategies are needed to improve both $CO_2$ conversion and liquid fuel yield during $CO_2$-FTS process. A steady-state model based on first principles and a modified Anderson-Schulz-Flory (ASF) distribution was developed for the $CO_2$-FTS process to predict gasoline range hydrocarbons ($C_5$-$C_{11}$). The model was implemented in Aspen Plus® using Fortran® routines and model validation was performed for different $H_2/CO_2$ feed ratios. Two process configurations (including a three-stage reactor in series and a single reactor with recycle) were considered for $CO_2$-FTS performance analysis and improvement through ex-situ water removal. Both $CO_2$-FTS process configurations showed significant improvements in $CO_2$ conversion (from 34 to above 70%) with up to 61.0% gasoline yield. Though the single reactor with recycle achieved a higher $CO_2$ conversion and gasoline production rate than the 3-stage reactor in series, the comparative analysis at the same $CO_2$ conversion of 71.5% revealed that both process configurations have a similar process efficiency of roughly 66.4%.

## 1. Introduction

### 1.1. Background

Within the current global industry, energy represents one of the most important requirements for daily life and activities including transportation, electricity, heating and cooling [1]. Looking specifically at transportation fuels, the demand was estimated at 54.5 million bbl/day in 2020. This is particularly true for gasoline whose demand is forecast to reach 27.7 million bbl/day in 2030 [2]. Since transport fuels are mostly produced from fossil fuels, they account for 36 % of $CO_2$ emissions worldwide which is predicted to increase by 22 % before 2040 [3].

It has been widely recognised that $CO_2$ emissions considerably contribute to climate change and global warming [4]. As a result, the Intergovernmental Panel on Climate Change (IPCC) recommends decreasing $CO_2$ emissions to limit the global temperature to 1.5 °C. Furthermore, the UK committed to achieve net-zero emissions by 2050 [5]. A transition to $CO_2$-free forms of energy thus, stopping the use of fossil fuels altogether seems desirable for a simplistic solution. However, this transition would profoundly disrupt the current economy owing to the limited capacity of electric vehicles and the intermittency of renewable energies such as wind and solar power [6,7].

Since decarbonizing the world transport industry which relies on fossil fuels could take several decades, it would be reasonable to undertake in parallel the synthesis of carbon–neutral fuels that will reduce fossil $CO_2$ emissions into the atmosphere. In this context, $CO_2$-neutral fuels arise as a potential solution wherein atmospheric $CO_2$ is captured and re-used for the synthesis of transport fuels leading to a closed $CO_2$-fuels-$CO_2$ cycle [6,8].

$$nCO + (2n+1)H_2 \quad C_nH_{2n+2} + nH_2O \tag{1}$$

$$nCO + 2nH_2 \rightarrow C_nH_{2n} + nH_2O \tag{2}$$

$$nCO + (2n-1)H_2 \rightarrow C_nH_{2n+1}OH + (n-1)\ H_2O \tag{3}$$

$$CO_2 + H_2 \rightleftharpoons CO + H_2O \tag{4}$$

The Fischer-Tropsch synthesis (FTS) process refers to as a polymerization process in which hydrocarbon (HC) chains are synthesised from a

---

* Corresponding author.
*E-mail address:* Meihong.Wang@sheffield.ac.uk (M. Wang).

https://doi.org/10.1016/j.cej.2023.142048
Received 30 October 2022; Received in revised form 10 January 2023; Accepted 19 February 2023

**Nomenclatures**

| | |
|---|---|
| b | Carbon number at break point |
| c | Olefin desorption rate constant |
| $f_1$ and $f_2$ | fractions of hydrocarbons on each side of carbon break point |
| $HHV_i$ | Higher heating value of component *i* (MW) |
| $k_i$ | Kinetic constant of hydrocarbon *i* formation |
| $\overline{M}$ | Average molecular weight of hydrocarbon mixture |
| $M_i$ | Molecular weight of hydrocarbon i |
| $\dot{N}_{HC}$ | Total molar flowrate of produced hydrocarbons (kmol/hr) |
| $\dot{n}_{HC_i}$ | Molar flowrate of hydrocarbon *i* (kmol/hr) |
| $P_i$ | Power utilisation in process *i* (MW) |
| $S_i$ | Selectivity of component *i* |
| $W_i$ | Weight fraction of component *i* |
| $X_i$ | Conversion of reactant *i* |
| $x_i$ | Mole fraction of component *i* |
| $Y_i$ | Yield of hydrocarbon *i* (%) |

*Greek letters*

| | |
|---|---|
| $\alpha$ | Chain growth probabilities |
| $\eta$ | Process efficiency (%) |
| $\lambda$ | Fitting parameter |

*Abbreviations*

| | |
|---|---|
| ASF | Anderson Schulz Flory |
| CAPEX | Capital expenditures |
| FBR | Fixed-bed reactor |
| FTS | Fischer-Tropsch synthesis |
| HC | Hydrocarbon |
| HHV | Higher heating value |
| INL | Idaho National Laboratory |
| IPCC | Intergovernmental Panel on Climate Change |
| OPEC | Organization of the Petroleum Exporting Countries |
| OPEX | Operational expenditures |
| RON | Research octane number |
| RWGS | Reverse water gas shift |
| SOEC | Solid oxide electrolysis cell |
| TEA | Technical and economic analysis |

carbon source via CO hydrogenation. The possible FTS reactions are described by Reactions (1) to (3) for alkanes, olefins and alcohols production from syngas respectively [9]. The synthesis of $C_{2+}$ HCs from $CO_2$ is usually performed in multiple reactors wherein $CO_2$ is first converted into syngas followed by the FTS process as illustrated in Fig. 1. The direct one-reactor method, also called modified $CO_2$-FTS process combines $CO_2$ reduction to syngas through the reverse water gas shift (RWGS) Reaction (4) and CO hydrogenation to HCs via FTS in a single reactor [10,11].

### 1.2. Previous studies on direct $CO_2$-FTS process for liquid fuel synthesis

The direct $CO_2$ conversion into HCs via the modified FTS process has recently gained much attention due to its ease of operation. Similar to the traditional FTS process, products from the modified $CO_2$-FTS process can be wide depending on the catalyst type, composition and structure. This paper focuses on the synthesis of liquid HCs ($C_{5+}$).

### 1.2.1. Rigs for direct $CO_2$-FTS and experimental studies

In comparison to the traditional FTS process, $CO_2$ conversion via the modified $CO_2$-FTS process is more challenging not only due to $CO_2$ thermodynamic stability but also because the RWGS reaction is endothermic ($\Delta H_{573K} = 38$ kJ/mol) hence requires higher temperatures whereas, FTS reactions are exothermic ($\Delta H_{573K} = -166$ kJ/mol) and high temperatures tend to favour light HCs [10,13]. Therefore, efficient catalysts should be active for both RWGS and FTS reactions under the same operating conditions [10].

Table 1 summarises a few studies on the $CO_2$-FTS process to liquid fuels performed at lab-scale. All experiments were carried out using FBRs with an inner diameter between 6.0 and 14.0 mm and up to 450 mm in height. Although up to 84.8 % $C_{5+}$ selectivity has been achieved, the yield of liquid fuels was found below 29.0 % due to low $CO_2$ conversion. It was reported that low $CO_2$ conversion during the $CO_2$-FTS process arises from excessive water produced from both RWGS and FTS reactions which negatively affect RWGS reaction rates [23,24]. To date, no plants either at pilot scale or at commercial scale of the modified $CO_2$-FTS process for liquid fuel synthesis have been reported in the open literature.

### 1.2.2. Modelling/simulation, optimisation and TEA studies

Meiri et al. [25] proposed a kinetic model for $CO_2$-FTS process simulation in CHEMCAD. They aimed to assess the effects of reactor configuration on $CO_2$ conversion, $CH_4$ and $C_{5+}$ selectivities. Their study demonstrated the importance of water removal to achieve higher $CO_2$-FTS reaction rates and $C_{5+}$ selectivity. A 1-D steady-state model of a membrane reactor for the $CO_2$-FTS process was developed by Najari et al. [26]. The model was based on mass and heat conservation and was used to investigate the effects of in-situ water removal through a

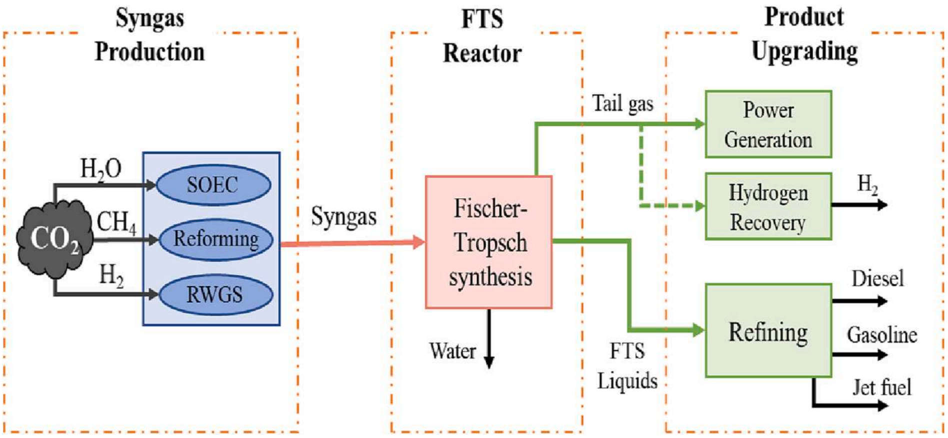

Fig. 1. Block flow diagram of a typical FTS plant, adapted from GSTC [12].

**Table 1**
Summary of studies performed for $CO_2$-FTS process to liquid fuels at lab-scale.

| Reactor type | Reactor diameter (mm) | $H_2/CO_2$ (mol/mol) | Catalyst | Operating T and P | $X_{CO2}$ (mol %) | Selectivity (%) | | $C_{5+}$ yield in mole (%) | Reference |
|---|---|---|---|---|---|---|---|---|---|
| | | | | | | $CH_4$ | $C_{5+}$ | | |
| FBR | N/A | 3.0 | $CuFeO_2$-6 | 300 °C and 10 bar | 17.3 | 2.7 | 66.3 | 11.5 | [14] |
| FBR | 14.0 | 1.0 | Na-$Fe_3O_4$/HZSM-5 | 320 °C and 30 bar | 22.0 | 4.0 | 78.0 | 17.2 | [15] |
| FBR | 10.0 | 3.0 | Fe-K/SiC | 300 °C and 25 bar | 41.7 | 10.3 | 56.0 | 23.4 | [16] |
| FBR | N/S | 3.0 | Co-Cu/$TiO_2$ | 240 °C and 50 bar | 18.4 | 26.1 | 42.1 | 7.7 | [17] |
| FBR | 7.0 | 2.7 | Co/MIL-53(Al) | 260 °C and 30 bar | 25.3 | 35.2 | 35.0 | 8.9 | [18] |
| FBR | 14.0 | 2.0 | Na-$Fe_3O_4$/HMCM-22 | 320 °C and 30 bar | 26.0 | 8.0 | 74.0 | 19.2 | [19] |
| FBR | N/S | 1.0 | $Co_6/MnO_x$ | 200 °C and 40 bar | 15.3 | N/S | 53.2 | 8.1 | [13] |
| FBR | 7.4 | 3.0 | Fe-K/MPC | 300 °C and 25 bar | 50.6 | 15.4 | 44.5 | 22.5 | [20] |
| FBR | 6.0 | 3.0 | Na-Fe@C/ HZSM-5–0.2 | 320 °C and 30 bar | 33.3 | 4.8 | 84.8 | 28.2 | [21] |
| FBR | 10.0 | 3.0 | Fe-Mn-K | 320 °C and 30 bar | 38.2 | 10.4 | 61.9 | 22.3 | [22] |

hydrophilic membrane on $CO_2$ conversion and hydrocarbon selectivity at different operating conditions. No model validation was performed as membrane reactors have not yet been experimentally studied for the direct $CO_2$-FTS process.

A TEA study on direct $CO_2$ conversion to gasoline fuel at a commercial-scale was performed by Fernández-Torres et al. [7] using Aspen HYSYS®. The authors aimed to investigate tail gas oxy-combustion for electricity generation using the Allam cycle, Rankine cycle and gas turbines to generate extra revenue for the $CO_2$-FTS plant. Their results indicated that the net electricity generation was 2.92, 1.95 and 2.06 kWh/L of gasoline when the $CO_2$-FTS plant is coupled with Allam cycle, Rankine cycle and gas turbines, respectively. Furthermore, for a gasoline production rate of 23.65 ton/hr, CAPEX and OPEX were estimated between 73 and 128 M$ and 244 to 1,951 M$/yr respectively [7].

### 1.3. *Aim and novel contribution of this paper*

The yield of liquid fuels (below 29 %) observed during $CO_2$-FTS process in experimental studies is still quite low for commercial applications. Though modelling and simulation approaches can help for process design and improvement at a lower cost [27], modelling/simulation studies on the direct $CO_2$-FTS process remain scarce. To the best of our knowledge, only two modelling studies are available in the open literature for $CO_2$-FTS process improvement via in-situ [26] and ex-situ [25] water removal. However, Najari et al. [26] focused on the $CO_2$-FTS process to gaseous HCs ($C_1$ to $C_4$). Although Meiri et al. [25] achieved up to 51 % $C_{5+}$ yield with 85 % $CO_2$ conversion, their kinetic model was based on experimental data with 45 to 78 % selectivity towards gaseous HCs. Since the improvement of $CO_2$-FTS process to liquid fuels has become more challenging from the catalyst design perspective [23], new strategies are therefore required to enhance both $CO_2$ conversion and $C_{5+}$ yield.

This work aims to investigate the technical performance of $CO_2$-FTS process to liquid fuels at a commercial-scale. In comparison with previous studies, especially Fernández-Torres et al. [7], a steady-state model for the $CO_2$-FTS process based on first principles and a modified ASF distribution to predict gasoline range hydrocarbons ($C_5$-$C_{11}$) is developed in this paper. The developed model is implemented in Aspen Plus® using Fortran® routines and validated using experimental data from Wei et al. [15]. Two $CO_2$-FTS process configurations (reactors in series vs a single reactor with recycle) are then considered for ex-situ water removal and their process performances are analysed and compared in terms of $CO_2$ conversion, gasoline yield, energy consumption and process efficiency.

## 2. Steady-state model development of the $CO_2$-FTS process

### 2.1. *Study of the $CO_2$-FTS process*

$CO_2$ and $H_2$ streams enter a fixed-bed reactor for gasoline fuel synthesis via the modified $CO_2$-FTS process. The general principle of the $CO_2$-FTS process is detailed in Section 1.1.

### 2.2. *Assumptions for model development*

The steady-state model of $CO_2$-FTS process was developed under the following assumptions:

- $CO_2$-FTS process operates at steady-state condition. Hence, heat and mass accumulations were not accounted for.
- $CO_2$-FTS model only focuses on reactant conversion and products from $CO_2$-FTS reactions based on material balance and reaction stoichiometry. However, the chain growth probability of hydrocarbons is specific to the type of reactor, catalyst and operating conditions [28,29].
- The type of hydrocarbons considered in this study only depends on the catalyst nature. Furthermore, oxygenated compounds were not favoured during experiments [15]. Therefore, products that can be obtained from Reaction (3) were neglected.
- The lumping technique was used to handle the infinite number of hydrocarbons from $CO_2$-FTS reactions. It is simply defined as grouping several components into a smaller number of components to represent the whole group [29].

### 2.3. *Modelling of $CO_2$-FTS process*

Most modelling/simulation, optimisation and TEA studies on the traditional FTS process used the Anderson–Schulz–Flory (ASF) theory to predict the distribution of hydrocarbons. The ASF model expresses the distribution of possible hydrocarbons in terms of their mass fractions ($W_i$) related to the corresponding carbon number $i$ and chain growth probability $\alpha$ (Eq. (5). However, experiments from Wei et al. [15] revealed that the direct $CO_2$-FTS process to liquid hydrocarbons does not follow the ASF distribution theory. A possible explanation could be the isomerisation, oligomerisation and aromatisation reactions taking place during the $CO_2$-FTS process in addition to the polymerisation reaction [10,15,30].

$$W_i = i \times (1-\alpha)^2 \times \alpha^{i-1} \tag{5}$$

Therefore, a modified version of the ASF theory was used to assess $CO_2$-FTS product distribution based on the one described by Donnelly et al. [31]. The modified ASF distribution considers two chain growth probabilities ($\alpha_1$ and $\alpha_2$) to evaluate the total product mass fraction for $i$ carbon number as shown in Eq. (6). It was assumed that each term in Eq.

(6) contributes equally at the breakpoint (with carbon number *b*) as described by Eq. (7). The fraction $f_2$ is then derived from Eq. (7) and calculated using Eq. (8).

$$W_i = f_1 \times {\alpha_1}^{i-1} + f_2 \times {\alpha_2}^{i-1} \tag{6}$$

$$W_b = 2 \times f_1 \times {\alpha_1}^{b-1} = 2 \times f_2 \times {\alpha_2}^{b-1} \tag{7}$$

$$f_1 \times {\alpha_1}^{b-1} = f_2 \times {\alpha_2}^{b-1} \Rightarrow f_2 = f_1 \times \left(\frac{\alpha_1}{\alpha_2}\right)^{b-1} \tag{8}$$

The sum of mass fractions for all carbon numbers is unity (Eq. (9). However, $C_2$ and $C_3$ compounds do not follow the theoretical ASF distribution [32–34]. Therefore, they are removed in the modified ASF model and their chain growth probabilities are calculated separately (Eqs. (10) and (11) based on the kinetic values proposed by Todic et al. [33] and adapted in this study for the $CO_2$-FTS process.

$$\sum_{i=1}^{\infty} W_i = \sum_{i=1}^{\infty} \left[f_1 \times {\alpha_1}^{i-1} + f_2 \times {\alpha_2}^{i-1}\right] = 1 \tag{9}$$

$$\alpha_{C_2} = \frac{k_1 P_{CO_2}}{k_1 P_{CO_2} + k_5 P_{H_2} + k_{6E} e^{2c}} \tag{10}$$

$$\alpha_{C_3} = \frac{k_1 P_{CO_2}}{k_1 P_{CO_2} + k_5 P_{H_2} + k_{6,0} e^{3c}} \tag{11}$$

After removing the mass fraction of $C_2$ and $C_3$ hydrocarbons, Eq. (9) becomes (12) for hydrocarbons with carbon number $i = 1$ and $i \geq 4$. Considering the sum of geometric series (Eq. (13) and substituting $f_2$ into Equations (12) and (13), the fraction $f_1$ can be evaluated using Eq. (14). Note that in Eq. (12), the term $[f_1 \bullet \alpha_1(1+\alpha_1) + f_2 \bullet \alpha_2(1+\alpha_2)]$ represents the sum of mass fraction $W_2$ and $W_3$, calculated using Eq. (6). A fitting parameter $\lambda$ was used in Eq. (14) to account for the aromatisation of light HCs [15,34].

$$\begin{aligned} \sum_{i=1,4}^{\infty} W_i &= \sum_{i=1}^{\infty} \left[f_1 \times {\alpha_1}^{i-1} + f_2 \times {\alpha_2}^{i-1}\right] - \left[f_1 \bullet \alpha_1(1+\alpha_1) + f_2 \bullet \alpha_2(1+\alpha_2)\right] \\ &= 1 - W_2 - W_3 \end{aligned} \tag{12}$$

$$\sum_{i=1}^{\infty} \left[f_1 \times {\alpha_1}^{i-1} + f_2 \times {\alpha_2}^{i-1}\right] = f_1[1/(1-\alpha_1)] + f_2[1/(1-\alpha_2)] \tag{13}$$

$$f_1 = \lambda \frac{1 - W_2 - W_3}{[1/(1-\alpha_1)] - \alpha_1 \bullet (1+\alpha_1) + [(1/(1-\alpha_2)) - \alpha_2 \bullet (1+\alpha_2)](\alpha_1/\alpha_2)^{b-1}} \tag{14}$$

Nevertheless, even the modified ASF distribution model does not consider any difference among components with the same carbon number. Hence, distinctions within the same carbon cuts were taken into consideration based on the catalyst characteristics. In this study, Na-$Fe_3O_4$/HZSM-5 catalyst was considered leading to five types of hydrocarbons including *n*-paraffins, isoparaffins, olefins, naphthenes and aromatics [15]. Since hydrocarbon distributions are based on their selectivity in C-mole %, the mass fraction obtained from the modified ASF theory is converted into their corresponding selectivity ($S_i$) using Equations (15) to (17). Selectivities are then distributed to each hydrocarbon type for a given carbon number based on catalyst features as provided by Wei et al. [15].

$$x_i = \frac{W_i}{M_i} \times \overline{M} \tag{15}$$

$$\frac{1}{\overline{M}} = \sum_{i=1}^{n} \frac{W_i}{M_i} \tag{16}$$

$$S_i = \frac{x_i \times i}{\sum_{i=1}^{n} x_i \times i} = \frac{\dot{n}_{HC_i} \times i}{\sum_{i=1}^{n} \dot{n}_{HC_i} \times i} \tag{17}$$

The $CO_2$-FTS reactor accomplishes several reactions including the RWGS reaction for $CO_2$ conversion followed by FTS reactions using produced CO (Table 2). The molar flowrate of each FTS reaction is calculated based on the stoichiometry and carbon mole balance as follows [29]:

$$\frac{\dot{n}_{CO_{in}}}{i} \times X_{CO_i} = \dot{n}_{HC_i} \tag{18}$$

Eq. (18) is re-arranged as (19) and applied to all FTS reactions taking place to evaluate the sum as given by Eq. (20). Where, $\sum_{i=1}^{n} i \times \dot{n}_{HC_i}$ represents the total molar flowrate of produced hydrocarbons and $\sum_{i=1}^{n} X_{CO_i}$ is the total CO conversion. Therefore, Eq. (20) is re-written as Eq. (21).

$$i \times \dot{n}_{HC_i} = X_{CO_i} \times \dot{n}_{CO_{in}} \tag{19}$$

$$\sum_{i=1}^{n} i \times \dot{n}_{HC_i} = \dot{n}_{CO_{in}} \times \sum_{i=1}^{n} X_{CO_i} \tag{20}$$

$$\dot{N}_{HC} = X_{CO} \times \dot{n}_{CO_{in}} \tag{21}$$

The same principle is applied to the RWGS reaction to assess $\dot{n}_{CO_{in}}$ as shown by Eq. (22). Equations (21) and (22) are combined to obtain Eq. (23) which is then applied to Eq. (17) to calculate the molar flowrate of each produced hydrocarbon from FTS reactions as shown by Eq. (24).

$$\dot{n}_{CO_{in}} = \dot{n}_{CO_{out}}\Big)_{RWGS} = X_{CO_2} \times \dot{n}_{CO_{2in}} \tag{22}$$

$$\dot{N}_{HC} = X_{CO} \times X_{CO_2} \times \dot{n}_{CO_{2in}} \tag{23}$$

$$\dot{n}_{HC_i} = \frac{S_i}{i} \times \dot{N}_{HC} \tag{24}$$

## 3. $CO_2$-FTS model implementation

The implementation of $CO_2$-FTS model was carried out in Aspen Plus® software using Peng-Robinson as the property method. Fig. 2 illustrates the $CO_2$-FTS process flowsheet developed in this work. It was assumed that $H_2$ and $CO_2$ are both available at standard conditions. $H_2$ and $CO_2$ streams are initially compressed to the desired pressure using a

**Table 2**
$CO_2$-FTS carbon range, selected components and chemical reactions.

| Carbon range | Product category | Model *i* | Component | Chemical reaction |
|---|---|---|---|---|
| $i = 1$ | CO | 1 | CO | $CO_2 + H_2 \rightarrow CO + H_2O$ |
| | Methane | | Methane | $CO + 3H_2 \rightarrow CH_4 + H_2O$ |
| $2 \leq i \leq 4$ | Light HCs | 3 and 4 | Propane | $3CO + 7H_2 \rightarrow C_3H_8 + 3H_2O$ |
| | | | Propene | $3CO + 6H_2 \rightarrow C_3H_6 + 3H_2O$ |
| | | | i-Butane | $4CO + 9H_2 \rightarrow i\text{-}C_4H_{10} + 4H_2O$ |
| $5 \leq i \leq 11$ | Gasoline | 8 | *n*-Octane | $8CO + 17H_2 \rightarrow n\text{-}C_8H_{18} + 8H_2O$ |
| | | | i-Octane | $8CO + 17H_2 \rightarrow i\text{-}C_8H_{18} + 8H_2O$ |
| | | | Octene | $8CO + 16H_2 \rightarrow C_8H_{16} + 8H_2O$ |
| | | | CycloOctane | $8CO + 16H_2 \rightarrow c\text{-}C_8H_{16} + 8H_2O$ |
| | | | Xylene | $8CO + 13H_2 \rightarrow C_8H_{10} + 8H_2O$ |
| $i \geq 12$ | Wax | 20 | Icosane | $20CO + 41H_2 \rightarrow C_{20}H_{42} + 20H_2O$ |

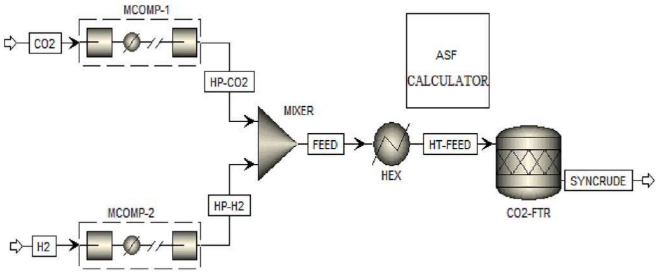

**Fig. 2.** Flowsheet of $CO_2$-FTS process in Aspen Plus®.

4-stage compressor with intercooling. The compressed gases are then mixed and heated to the reactor operating temperature. Afterwards, the resulting stream (HT-FEED) is sent to the $CO_2$-FTS reactor. The $CO_2$-FTS reactor is represented as a stoichiometry reactor block ($CO_2$-FTR) and Fortran® routines were used to assess the distribution of hydrocarbons. Table 3 recapitulates the equations implemented in Aspen Plus®.

The modified ASF distribution model was first calculated in a separate spreadsheet for every carbon number ranging from 1 to 50. In order to handle the wide range of possible components in the model, lumping of components was performed as summarised in Table 2. For each carbon range, a specific carbon number and corresponding hydrocarbons were chosen to represent the product category. Then considering Table 3, Fortran® routines evaluate the molar flowrate of each chemical reaction accomplished by the stoichiometry reactor block.

## 4. $CO_2$-FTS model validation

The $CO_2$-FTS model was validated using data from experiments conducted at Dalian National Laboratory for Clean Energy in China [15]. Details on the experimental $CO_2$-FTS reactor are elaborated in Section 1.2.1 (Table 1). Six sets of experiments were carried out to assess the hydrocarbon selectivities for different $H_2/CO_2$ feed ratios. Data using $H_2/CO_2$ ratios of 1.0 and 3.0 were selected for the model validation. This is because they achieved more than 70 % selectivity towards gasoline-range hydrocarbons.

The input process conditions and parameters used for the $CO_2$-FTS model validation are given in Table 4. Not all required data were available from Wei et al. [15]. Thus, some parameters were assumed based on available literature as detailed in Table 4. The validation results are provided in terms of hydrocarbons and CO selectivities (in C-mole%) for different $H_2/CO_2$ ratios. Fig. 3a and 3b show good agreement between experimental data and model predictions for both $H_2/CO_2$ feed ratios.

The relative errors between model predictions and experimental values for each product category were also calculated and they are in Table 5. For $H_2/CO_2$ ratios of 1.0 and 3.0, relative errors were found below 9.0 % and 7.0 % respectively. Therefore, the $CO_2$-FTS model developed in Aspen Plus® using Fortran® routines can reasonably predict the gasoline-range hydrocarbons ($C_5$-$C_{11}$) and can be used for further performance analysis.

**Table 3**
Summary of $CO_2$-FTS mathematical modelling.

| Parameter | Equation |
|---|---|
| Growth probability of $C_2$ component | Equation (10) |
| Growth probability of $C_3$ component | Equation (11) |
| Product fraction related to $\boldsymbol{\alpha}_1$ | Equation (14) |
| Product fraction related to $\boldsymbol{\alpha}_2$ | Equation (8) |
| Mass fraction of hydrocarbon $i$ | Equation (6) |
| Average molecular weight of HCs | Equation (16) |
| Mole fraction of component $i$ | Equation (15) |
| Selectivity of component $i$ | Equation (17) |
| Total molar flowrate of HCs | Equation (23) |
| Molar flowrate of hydrocarbon $i$ | Equation (24) |

**Table 4**
Input parameters for $CO_2$-FTS model validation.

| Parameter | Value | Reference | |
|---|---|---|---|
| Reactor temperature (°C) | 320 | [15] | |
| Reactor pressure (bar) | 30 | | |
| $H_2/CO_2$ ratio (mol basis) | 3.0 | 1.0 | |
| Inlet $H_2$ and $CO_2$ temperature (°C) | 25 | | |
| Inlet $H_2$ and $CO_2$ pressure (bar) | 1 | | |
| Inlet feed flowrate | 4.0 L/hr | | |
| $CO_2$ conversion | 0.34 | 0.22 | |
| Chain growth probability | $\alpha_1$ | 0.75 | [31] |
| | $\alpha_2$ | 0.82 | |
| Carbon number at break point | 7 | | |
| Kinetic constants | $k_1$ | $1.66 \times 10^{-2}$ | [33] |
| | $k_5$ | $6.99 \times 10^{-4}$ | |
| | $k_{6,0}$ | $2.02 \times 10^{-2}$ | |
| | $k_{6E}$ | $7.62 \times 10^{-5}$ | |
| Constant c | $-0.26$ | | |
| Fitting parameter λ<br>$i \geq 5, 0.06e^{0.48i}$ | $i \leq 4, 0.22e^{0.34i}$<br>[33,34] | | |

## 5. Performance analysis of $CO_2$-FTS process for gasoline fuel synthesis

### 5.1. Assumptions and evaluation criteria for $CO_2$-FTS performance analysis

$CO_2$-FTS performance analysis was performed under the following assumptions:

- Although the $CO_2$-FTS model validation was performed at a laboratory-scale, process analysis was carried out at industrial-scale under the assumptions that both $CO_2$-FTS reactor and Na-$Fe_3O_4$/HZSM-5 catalyst behave the same way at lab-scale and industrial-scale.
- $CO_2$ and $H_2$ inlet flowrates were assumed to be 110.02 and 15.12 ton/hr respectively. These values were chosen to achieve a commercial $CO_2$-FTS plant capacity of 4500 bbl/day [7].
- $CO_2$-FTS process performance is given in terms of $CO_2$ conversion, gasoline yield, energy consumption and process efficiency.
- $CO_2$-FTS process efficiency and gasoline yield were calculated using Eqs. (25) and (26) respectively. The $CO_2$-FTS process efficiency considers the high heating values (HHV) of gasoline fuel and feed gases as well as the required energy of each operation units [28,35].

$$\eta_{CO_2-FTS} = \frac{HHV_{gasoline}}{HHV_{in} + P_{CO_2-FTS}} \tag{25}$$

$$Y_{gasoline} = X_{CO_2} \times S_{gasoline} \tag{26}$$

$$X_{CO_2} = \frac{\dot{n}_{CO_2 in} - \dot{n}_{CO_2 out}}{\dot{n}_{CO_2 in}} \tag{27}$$

- Except for the base case of $CO_2$-FTS process which has a fixed $CO_2$ conversion as specified by Wei et al. [15], $CO_2$ conversion in the remaining case studies was assessed using Eq. (27).
- Given the current maturity of fixed-bed reactors, 5 % heat losses were assumed during calculations of the $CO_2$-FTS process efficiency [9].
- For all case studies, no pressure drop was assumed in the heaters and coolers.

### 5.2. $CO_2$-FTS process performance using a single reactor

#### 5.2.1. Justification for this case study

The $CO_2$-FTS process using a single reactor features an open-loop

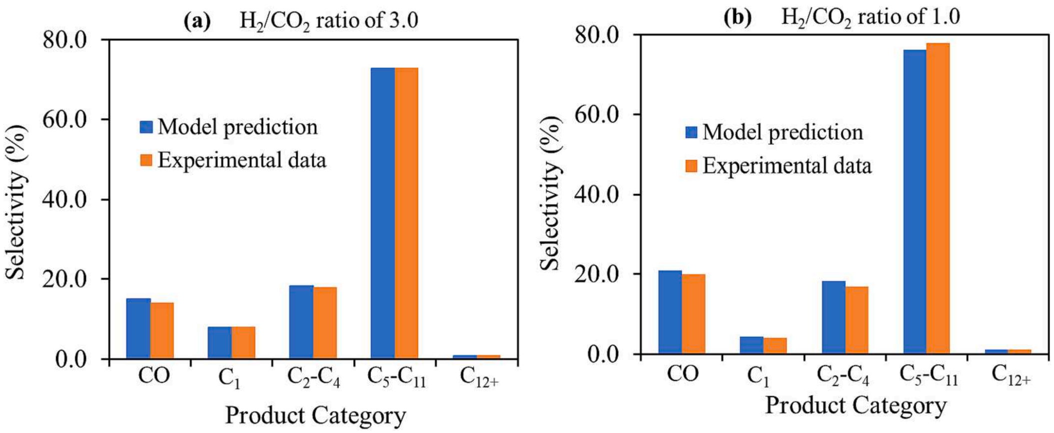

**Fig. 3.** Model predictions and experimental values of $CO_2$-FTS product selectivities for different $H_2/CO_2$ feed ratios.

**Table 5**

Relative errors between model predictions and experimental values of $CO_2$-FTS product selectivities.

| Product category | Relative errors (%) | |
|---|---|---|
| | $H_2/CO_2$ of 3.0 | $H_2/CO_2$ of 1.0 |
| CO | 6.65 | 4.50 |
| $CH_4$ | 1.38 | 7.00 |
| $C_2$-$C_4$ | 1.60 | 8.93 |
| $C_5$-$C_{11}$ | 0.16 | 2.18 |
| $C_{12+}$ | 6.97 | 6.67 |

configuration without the recirculation or upgrade of unconverted reactants, water removal and/or reactor design. It is referred to as base case and the obtained results were used as a reference for performance comparison between the base case and optimised plants. The study of the base case for $CO_2$-FTS plant was necessary to evaluate the performance of each operation unit, especially the $CO_2$-FTS reactor block.

### 5.2.2. Set-up of this case study

The process simulation of the base case for gasoline fuel synthesis through $CO_2$-FTS process is displayed in Fig. 4a. In the base case, the syncrude stream leaving the $CO_2$-FTS reactor is first cooled down to 40 °C based on the temperature performance of industrial coolers [25]. The resulting stream (SYN-2) is then separated into three streams using a three-phase outlet flash drum: light gas stream (containing unconverted feed gases and light hydrocarbons), gasoline stream (mostly $C_5$-$C_{11}$ hydrocarbons) and water stream. The remaining operating conditions of the $CO_2$-FTS process to gasoline are the same as presented in Table 4 for the $H_2/CO_2$ ratio of 3.0.

### 5.2.3. Results and discussion of this case study

The overall material balance and energy input of the base case for the $CO_2$-FTS plant is presented in Fig. 4b. The characteristics of the produced gasoline as well as the process performance were verified, and the results are presented in Table 6. The gasoline fuel has a density of 767.1 kg/$m^3$ and a research octane number (RON) of 94.6 which is between the current gasoline RON grade range of 80 to 110 [36]. The base case of $CO_2$-FTS process plant leads to roughly 6.1 ton/hr of gasoline fuel, 28.0 ton/hr of water and 91.1 ton/hr of light gas. The total energy required was evaluated at 155.4 MW which resulted in a $CO_2$-FTS process efficiency of approximately 39.0 %.

The $CO_2$-FTS process achieves a gasoline selectivity of 72.9 % with methane selectivity below 8.0 % which agrees with the experimental results when using Na-$Fe_3O_4$/HZSM-5 catalyst for direct $CO_2$ conversion into gasoline fuel [15]. Furthermore, the direct $CO_2$-FTS process results in roughly 1.0 % selectivity towards $C_{12+}$ hydrocarbons (Fig. 3) based on

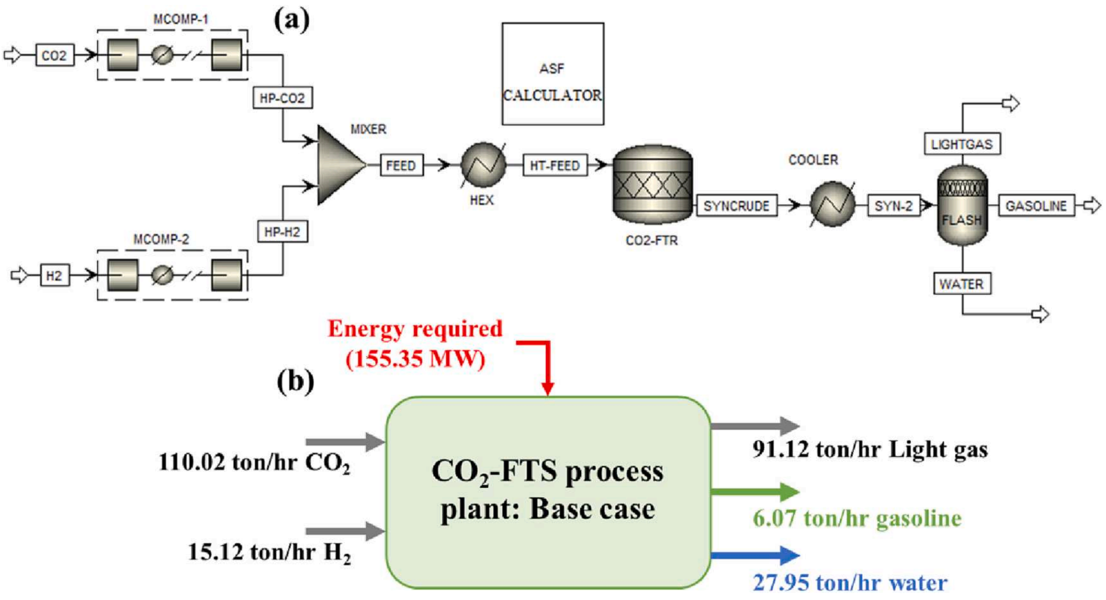

**Fig. 4.** (a) Process simulation of the base case for $CO_2$-FTS plant and (b) overall material (mass) balance and total energy input.

**Table 6**
Performance summary of the $CO_2$-FTS preliminary process design.

| Parameter | | Value |
|---|---|---|
| Gasoline fuel features | Mass flowrate (ton/hr) | 6.07 |
| | Density ($kg/m^3$) | 767.13 |
| | RON | 94.56 |
| | HHV (MW) | 75.88 |
| Energy consumption (MW) | Feed compressors | 70.79 |
| | Feed heater | 10.86 |
| | Reactor cooling jacket | 22.53 |
| | Syncrude cooler | 43.20 |
| | Flash drum | 0.57 |
| | Heat losses (5 %) | 7.40 |
| Conversion (mol%) | $CO_2$ | 34.00 |
| | CO | 85.35 |
| Gasoline yield in mole (%) | | 24.78 |
| $CO_2$-FTS process efficiency (%) | | 38.96 |

Na-$Fe_3O_4$/HZSM-5 catalyst characteristics. Therefore, a distillation column was not required for the syncrude upgrade to liquid fuels. However, the gasoline yield is only 24.8 % due to low $CO_2$ conversion (approximately 34.0 %). The results also indicate that the light gas stream (Fig. 4) contains 72.4 ton/hr and 10.4 ton/hr of $CO_2$ and $H_2$ mass flowrate respectively which account for more than 90 % of the total light gas flowrate. It will be shown in the next sections that the light gases can be re-used to optimise the $CO_2$-FTS process performance.

## 5.3. $CO_2$-FTS process performance using multiple reactors in series

### 5.3.1. Justification for this case study

Water formation during direct $CO_2$ conversion into liquid fuels significantly decreases the driving force of the RWGS reaction, hence inhibits $CO_2$ conversion. Continuous and selective water removal is therefore essential to achieve a higher RWGS reaction rate and $CO_2$ conversion [23,24]. As a result, this study explores multiple $CO_2$-FTS reactors in series with interstage cooling for ex-situ water removal to assess the effects of the multi-stage reactor system on $CO_2$ conversion, gasoline yield, energy consumption and process efficiency.

### 5.3.2. Set-up of this case study

Fig. 5 depict the configuration concept of the $CO_2$-FTS process using multiple reactors in series and process simulation of a 2-stage $CO_2$-FTS reactor system in Aspen Plus®. A single $CO_2$-FTS reactor unit includes a heat exchanger, fixed-bed reactor (modelled as a stoichiometry reactor block), cooler and three-outlet flash drum. The aforementioned operation units operate as described in Sections 4 and 5.2.2.

The second feed stream (FEED-2), mostly containing unconverted $CO_2$, $H_2$ and CO, is then sent to the next $CO_2$-FTS reactor unit. Up to three reactors in series were studied. Each $CO_2$-FTS reactor uses Na-$Fe_3O_4$/HZSM-5 catalyst to accomplish the chemical reactions elaborated in Table 2 and Fortran® routines assess the molar flowrate of each reaction. Finally, a mixer is used to combine all gasoline streams leaving the flash drums. The operating conditions are the same as in Table 4 for the $H_2/CO_2$ ratio of 3.0. Moreover, each $CO_2$-FTS reactor unit operates under the same conditions.

### 5.3.3. Results and discussion of this case study

The overall material balance and total energy input for the $CO_2$-FTS plant using 3 reactors in series is presented in Fig. 6. Table 7 details the $CO_2$-FTS process performance using one reactor (base case) compared to two and three reactors in series.

The results show that using two $CO_2$-FTS reactors in series increases $CO_2$ conversion from 34.0 to 56.6 %. This leads to a gasoline yield of 41.6 % which is 1.7 times higher than that of the $CO_2$-FTS process with a

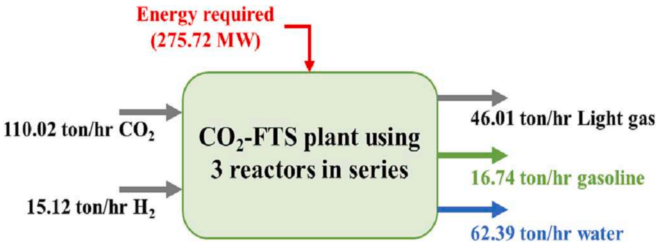

**Fig. 6.** Overall material (mass) balance and total energy input of $CO_2$-FTS process using three reactors in series.

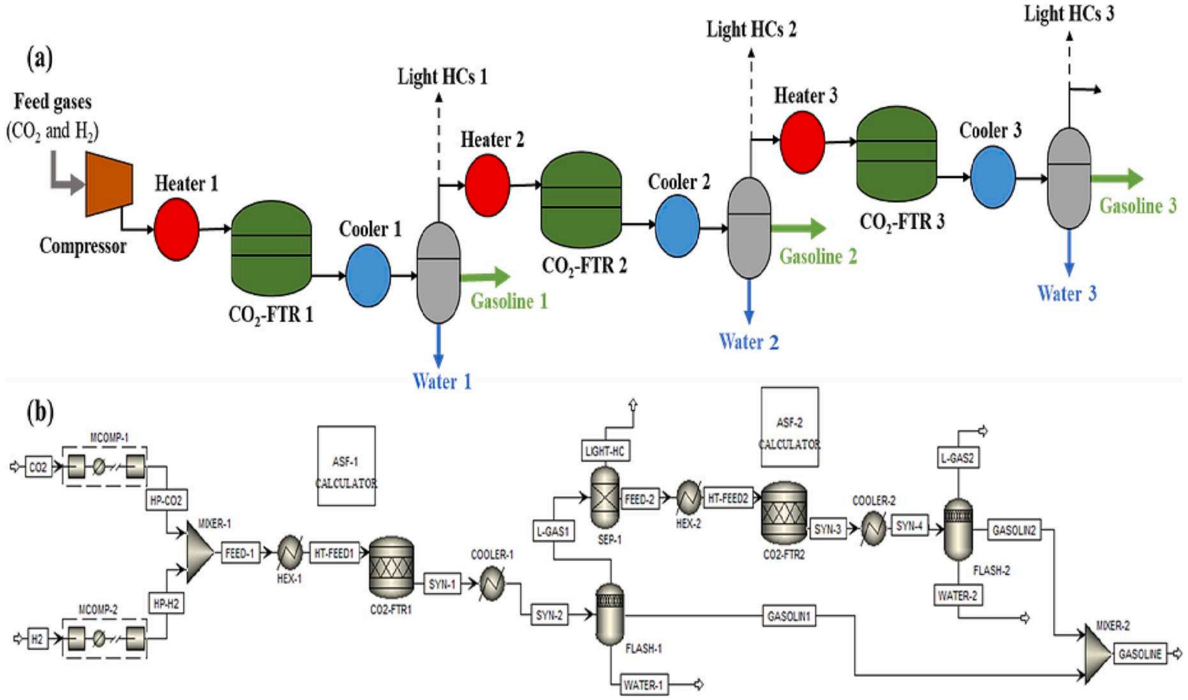

**Fig. 5.** (a) Configuration concept and (b) process simulation of $CO_2$-FTS to gasoline using multiple reactors in series.

**Table 7**
Performance summary of the $CO_2$-FTS process using multiple reactors in series.

| Parameter | | 1 reactor (base case) | 2 reactors in series | 3 reactors in series |
|---|---|---|---|---|
| Gasoline fuel features | Mass flowrate (ton/hr) | 6.07 | 11.33 | 16.74 |
| | Density (kg/$m^3$) | 767.13 | 766.15 | 765.77 |
| | HHV (MW) | 75.88 | 141.63 | 209.25 |
| Energy consumption (MW) | Feed compressors | 70.79 | 70.79 | 70.79 |
| | Feed heaters | 10.86 | 28.74 | 40.66 |
| | Reactor cooling jackets | 22.53 | 41.97 | 55.41 |
| | Syncrude coolers | 43.20 | 73.87 | 94.35 |
| | Flash drums | 0.57 | 1.05 | 1.38 |
| | Heat losses (5 %) | 7.40 | 10.82 | 13.13 |
| Conversion (mol %) | $CO_2$ | 34.00 | 56.63 | 71.54 |
| | CO | 85.35 | 92.94 | 96.18 |
| Gasoline yield in mole (%) | | 24.78 | 41.55 | 52.48 |
| $CO_2$-FTS process efficiency (%) | | 38.96 | 53.12 | 66.41 |

single reactor. Furthermore, $CO_2$-FTS plant using three reactors in series produces 16.7 ton/hr of gasoline with 52.5 % gasoline yield and a considerable increase in $CO_2$ conversion from 34.0 to 71.5 %.

These results are in good agreement with experimental findings using 2-stage [23] and 3-stage [37] fixed-bed reactors for direct $CO_2$ conversion into $C_{5+}$ hydrocarbons. The authors explained that water removal accelerates the formation of active carbide phases which are crucial for $CO_2$-FTS activity. Since RWGS reaction rates and modified ASF hydrocarbon distribution are quite similar in each $CO_2$-FTS reactor, the more $CO_2$-FTS reactors are set in series, the higher overall $CO_2$ conversion is achieved.

The analysis of $CO_2$-FTS energy consumption reveals that increasing the number of reactors results in higher energy requirements for the overall process plant. Indeed, the 2-stage and 3-stage $CO_2$-FTS reactor systems respectively consume 227.2 MW and 275.7 MW of energy which are 46.4 % and 77.6 % higher than the energy requirement of a single $CO_2$-FTS reactor unit. In both cases, syncrude coolers show the highest energy consumption accounting for 32.5 % (Fig. 7a) and 34.2 % (Fig. 7b) of energy usage for the 2-stage and 3-stage $CO_2$-FTS reactor systems, respectively.

The feed gas compressors have the second-highest share of energy consumption (31.2 % and 25.7 % of energy required in the 2-stage and 3-stage $CO_2$-FTS reactor systems respectively). For the same inlet flowrates, Fernández-Torres et al. [7] reported an energy consumption of 10.1 MW for the feed gas compression which is 85.8 % lower than the one observed in this work. This is simply because their study assumed that the feed gases are available to the $CO_2$-FTS plant at 25 bar. Hence, lower energy was required to compress the inlet gases to the reactor's desired pressure. Under similar assumptions, the feed gas compressors in this study would only need 6.2 % and 4.8 % of the total energy required in the 2-stage and 3-stage $CO_2$-FTS reactor systems respectively.

On the other hand, multiple $CO_2$-FTS reactors in series also lead to higher gasoline production rates. For example, the 3-stage $CO_2$-FTS reactor system reached 16.7 ton/hr gasoline production rate resulting in a process efficiency of 66.4 % which is nearly twice that of the single $CO_2$-FTS reactor unit. Therefore, it is sensitive to conclude that multi-stage reactors coupled with periodical water removal can help to achieve higher $CO_2$ conversion thus, higher gasoline yield and process efficiency.

### 5.4. $CO_2$-FTS process performance using a single reactor with recycle

#### 5.4.1. Justification for this case study

The natural alternative to multiple reactors in series is water removal followed by material recirculation so that unconverted feedstock can be re-used within the single $CO_2$-FTS reactor. This technique aims to enhance the overall process efficiency while limiting the net material consumption [35]. Since increasing the number of reactors showed noticeable effects on the $CO_2$-FTS process performance for gasoline synthesis, it is paramount to also understand the effects of material recycling (hence, recycle ratio) using a single $CO_2$-FTS reactor on $CO_2$ conversion, gasoline yield, energy consumption and process efficiency.

#### 5.4.2. Set-up of this case study

The configuration concept and flowsheet diagram of the $CO_2$-FTS process to gasoline using a single reactor with recycle developed in Aspen Plus® software is illustrated in Fig. 8. The top exit stream (L-GAS2) of the separator is first split into two flows (RECYCLE and L-GAS3 streams). Given the high cost of hydrogen, it is assumed that the L-GAS3 stream will be sent to an upgrade section so that excess/unreacted $H_2$ can be recovered for on or off-site purposes which could allow further plant optimisation. Although the $H_2$ recovery section is outside of the scope of this research, the HHV of $H_2$ was considered in the process efficiency calculation (Eq. (25)).

The RECYCLE stream (mostly containing $H_2$, CO and $CO_2$) is then sent to the feed mixer where it is combined with high-pressure $CO_2$ and $H_2$ feed streams. The remaining steps of the $CO_2$-FTS process to gasoline are as described in Section 5.2.2 for a single $CO_2$-FTS reactor unit. Note that the syncrude leaving the $CO_2$-FTS reactor ($CO_2$-FTR) is only cooled down before light gases (L-GAS1) are separated from water and gasoline. Since the heater and cooler were assumed not to have any pressure drop (Section 5.1), the pressure of the recycled gas stream (RECYCLE) remained the same as that of the feed gas. Therefore, no compressor for the recycled gas was needed in this simulation.

The recycle ratio (split fraction in the SPLITTER block) was initially

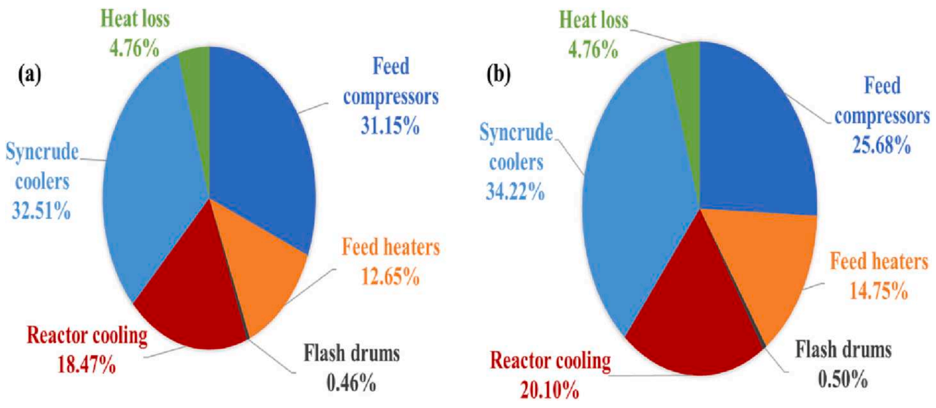

**Fig. 7.** Energy repartition of (a) two-stage and (b) three-stage $CO_2$-FTS process to gasoline.

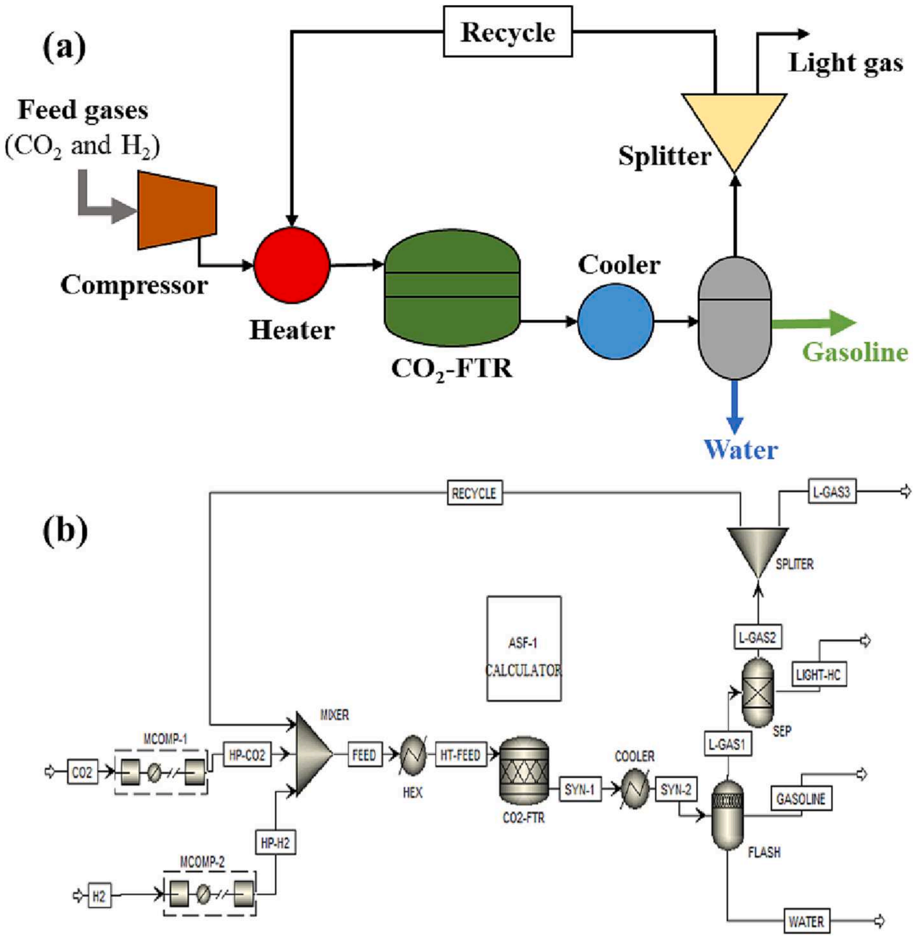

**Fig. 8.** (a) Configuration concept and (b) process simulation of $CO_2$-FTS to gasoline using a single reactor with recycle.

set to 0.5. The sensitivity analysis tool was then used in Aspen Plus® to assess the effects of the recycle ratio on $CO_2$ conversion and gasoline production. The remaining operating conditions are the same as in Table 4.

### 5.4.3. *Results and discussion of this case study*

The recycle ratio was varied from 0.0 to 0.9 given that not all unconverted reactants can be recycled back to the reactor. Moreover, for recycle ratios above 0.9, the sensitivity analysis results showed errors. This is because the system was no longer in mass balance due to $CO_2$ accumulation and its equilibrium conversion limitations [38].

Fig. 9 illustrates the effects of the recycle ratio on $CO_2$ conversion and gasoline yield. Although $CO_2$ conversion per pass through the reactor was set to 0.34 as per input data (Table 4), the results show a considerable increase in $CO_2$ conversion of the configured plant (therefore, gasoline yield) with the recycle ratio. Recirculating 90 % of unconverted reactants achieved 83.9 % $CO_2$ conversion which corresponds to roughly 61.2 % gasoline yield.

The overall material balance and total energy input for the $CO_2$-FTS plant using a single reactor with recycle (recycle ratio of 0.9) is illustrated in Fig. 10. The performance summary of the $CO_2$-FTS process to gasoline using a single reactor (base case) compared to a single reactor with a recycle ratio of 0.9 (recycle system) is detailed in Table 8.

It was found that the recycle system requires approximately 2.1 times more energy than the preliminary plant. The highest energy consumption of 112.4 MW is observed from the cooler located next to the $CO_2$-FTS reactor. This is simply due to the higher production rate observed in the recycle system. As a matter of fact, the gasoline production rate in the recycle system was close to 20.0 ton/hr (with a $CO_2$-FTS process efficiency of 69.6 %) which is more than 3 times that of the preliminary plant. Hence, water removal followed by reactant recirculation can effectively improve both $CO_2$ conversion and $CO_2$-FTS process efficiency.

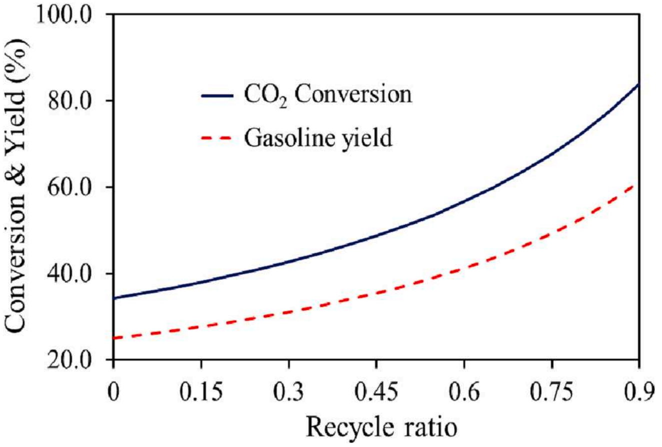

**Fig. 9.** Effects of the recycle ratio on $CO_2$ conversion and gasoline yield during $CO_2$-FTS process.

## 6. $CO_2$-FTS performance comparison between a single reactor with recycle and multiple reactors in series

The configured $CO_2$-FTS plants elaborated above, a single reactor

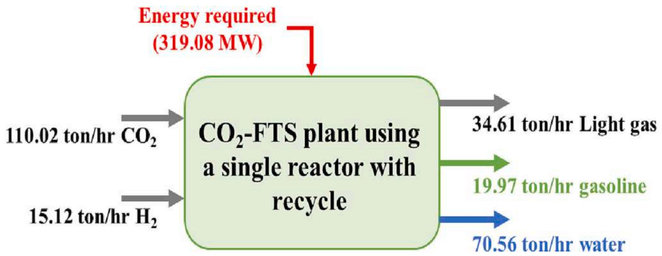

**Fig. 10.** Overall material (mass) balance and total energy input of $CO_2$-FTS process using a single reactor with recycle (recycle ratio of 0.9).

**Table 8**
Performance summary of the $CO_2$-FTS process using single reactor compared to single reactor with recycle.

| Parameter | | Base case | Recycle system |
|---|---|---|---|
| Gasoline fuel features | Mass flowrate (ton/hr) | 6.07 | 19.97 |
| | Density (kg/m$^3$) | 767.13 | 765.34 |
| | HHV (MW) | 75.88 | 249.63 |
| Energy consumption (MW) | Feed compressors | 70.79 | 70.79 |
| | Feed heaters | 10.86 | 51.56 |
| | Reactor cooling jackets | 22.53 | 66.84 |
| | Syncrude coolers | 43.20 | 112.42 |
| | Flash drums | 0.57 | 2.28 |
| | Heat losses (5 %) | 7.40 | 15.19 |
| Conversion (mol%) | $CO_2$ | 71.54 | 83.94 |
| | CO | 85.35 | 98.33 |
| Gasoline yield in mole (%) | | 24.78 | 61.18 |
| $CO_2$-FTS process efficiency (%) | | 38.96 | 69.64 |

with recycle and multiple reactors in series, have demonstrated the essential feature of enhancing $CO_2$ conversion and gasoline yield through ex-situ water removal from the system. A performance comparison between the two configuration systems (Tables 7 and 8) indicates that the single reactor with recycle (recycle ratio of 0.9) has a higher gasoline production rate than the three-stage reactors in series (20.0 and 16.7 ton/hr, respectively). Although the recycle system requires roughly 1.2 times more energy than the three-stage reactors in series, it achieves a higher process efficiency of 69.6 % due to increased gasoline production. A possible explanation could be the higher $CO_2$ conversion observed in the recycle system which also results in a higher gasoline yield.

However, it was previously demonstrated that the more $CO_2$-FTS reactors are set in series, the higher $CO_2$ conversion is achieved whereas, a lower recycle ratio would result in lower $CO_2$ conversion. Therefore, the two configuration systems are also compared at the same $CO_2$ conversion to identify which one would provide the best performance. The three reactors in series achieve a $CO_2$ conversion of 71.5 % hence, a recycle ratio of 0.8 was chosen (based on Fig. 9) to maintain the same $CO_2$ conversion in the recycle system.

Fig. 11 depicts the overall mass balance and total energy consumption of direct $CO_2$-FTS processes to gasoline fuel using three reactors in series (Fig. 11a) and a single reactor with recycle (Fig. 11b) for the same $CO_2$ conversion of 71.5 %. It can be seen that the gasoline production rate for both $CO_2$-FTS process plants is quite similar (16.74 and 16.94 ton/hr for the 3-stage reactor in series and single reactor with recycle respectively).

Although the recycle system had a slightly higher energy requirement than the 3-stage reactor in series (279.69 and 275.72 MW, respectively), similar $CO_2$-FTS process efficiency of roughly 66.4 % was found for both systems. Hence, in terms of $CO_2$ conversion and process efficiency, both configuration plants can effectively improve the $CO_2$-FTS process performance with more than 52 % gasoline yield. In industrial applications, this could reduce the operating costs for the disposal of by-products and/or management of unconverted reactants. Although the reported results show great improvement in the $CO_2$-FTS process performance, it is important to specify that more studies on economic analysis are also needed to provide further insights into the commercial deployment of the $CO_2$-FTS process.

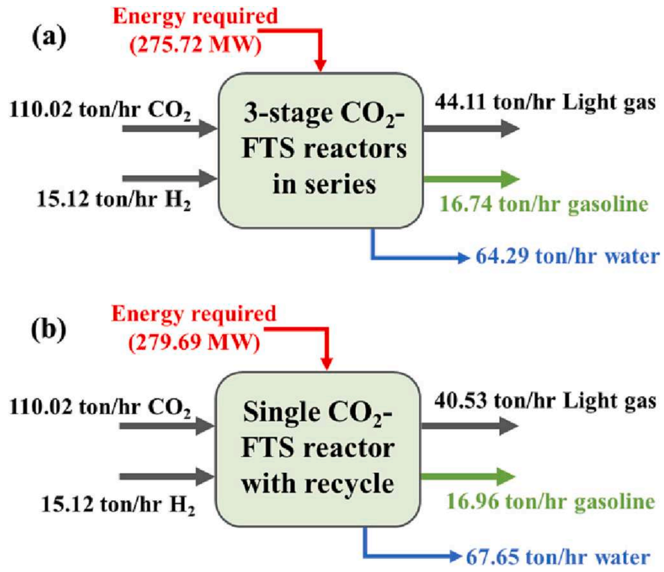

**Fig. 11.** Overall material (mass) balance and required energy of $CO_2$-FTS process using (a) three reactors in series and (b) single reactor with recycle for 71.5% $CO_2$ conversion.

## 7. Conclusion

In this paper, a steady-state $CO_2$-FTS model (in Aspen Plus® using Fortran® routines) was developed and validated. The model is based on first principles and a modified ASF distribution to predict gasoline range hydrocarbons ($C_5$-$C_{11}$). Model validation was performed for two sets of data with $H_2/CO_2$ feed ratios of 1.0 and 3.0. Two $CO_2$-FTS process configurations for ex-situ water removal (three-stage reactor in series and single reactor with recycle) were considered and their process performances were analysed and compared in terms of $CO_2$ conversion, gasoline yield, energy consumption and process efficiency.

Both $CO_2$-FTS process plants showed significant improvements in $CO_2$ conversion (from 34 to above 70 %) and gasoline yield (from 25 to over 52 %) through ex-situ water removal. A comparative analysis between the two direct $CO_2$-FTS process plants indicated that the single reactor with recycle (recycle ratio of 0.9) has a higher gasoline yield (around 61.0 %) and gasoline production rate (roughly 20.0 ton/hr) than the 3-stage reactor in series due to higher $CO_2$ conversion (about 84.0 %). However, the performance analysis at the same $CO_2$ conversion of 71.5 % revealed that both process configurations have a similar process efficiency of around 66.4 %. Therefore, under the investigated conditions, both $CO_2$-FTS process plants can successfully achieve higher gasoline yield and process efficiency.

## Declaration of Competing Interest

The authors declare that they have no known competing financial interests or personal relationships that could have appeared to influence the work reported in this paper.

## Data availability

No data was used for the research described in the article.

## Acknowledgments

The first author would like to thank the University of Sheffield for partial PhD scholarship. The second author would like to acknowledge the financial support of EU RISE project OPTIMAL (Ref 101007963).

## References

[1] I. Overland, Energy: The missing link in globalization, Energy Res. Soc. Sci. 14 (2016) 122–130, https://doi.org/10.1016/J.ERSS.2016.01.009.

[2] Sönnichsen N. Demand outlook for selected oil products worldwide from 2020 to 2045 2022. https://www.statista.com/statistics/282774/global-product-demand-outlook-worldwide (accessed February 27, 2022).

[3] OPEC. World oil outlook 2040. Vienna: 2017.

[4] A.A. Khozema, I.A. Mardiana, Y. Yusri, Issues, impacts, and mitigations of carbon dioxide emissions in the building sector, Sustainability 12 (2020) 7427, https://doi.org/10.3390/SU12187427.

[5] IPCC. Special report - Global Warming of 1.5 $^{o}$C 2018:300. https://www.ipcc.ch/sr15 (accessed November 5, 2021).

[6] B.R. de Vasconcelos, J.M. Lavoie, Recent advances in power-to-X technology for the production of fuels and chemicals, Front. Chem. 7 (2019) 392, https://doi.org/10.3389/fchem.2019.00392.

[7] M.J. Fernández-Torres, W. Dednam, J.A. Caballero, Economic and environmental assessment of directly converting CO2 into a gasoline fuel, Energy Convers Manag 252 (2022), 115115, https://doi.org/10.1016/j.enconman.2021.115115.

[8] R. Rosa, The role of synthetic fuels for a carbon neutral economy, C- J Carbon Res 3 (2017) 11, https://doi.org/10.3390/c3020011.

[9] S. Saeidi, M.K. Nikoo, A. Mirvakili, S. Bahrani, N.A. Saidina Amin, M. R. Rahimpour, Recent advances in reactors for low-temperature Fischer-Tropsch synthesis: Process intensification perspective, Rev. Chem. Eng. 31 (2015) 209–238, https://doi.org/10.1515/revce-2014-0042.

[10] R.P. Ye, J. Ding, W. Gong, M.D. Argyle, Q. Zhong, Y. Wang, et al., CO2 hydrogenation to high-value products via heterogeneous catalysis, Nat. Commun. 10 (2019) 5698, https://doi.org/10.1038/s41467-019-13638-9.

[11] W. Li, H. Wang, X. Jiang, J. Zhu, Z. Liu, X. Guo, et al., A short review of recent advances in CO2 hydrogenation to hydrocarbons over heterogeneous catalysts, RSC Adv. 8 (2018) 7651–7669, https://doi.org/10.1039/c7ra13546g.

[12] GSTC. Syngas applications - Synthetic Fuels 2022. https://globalsyngas.org/syngas-technology/syngas-applications/synthetic-fuels/ (accessed January 28, 2022).

[13] Z. He, M. Cui, Q. Qian, J. Zhang, H. Liu, B. Han, Synthesis of liquid fuel via direct hydrogenation of CO2, PNAS 116 (2019) 12654–12659, https://doi.org/10.1073/pnas.1821231116.

[14] Y.H. Choi, Y.J. Jang, H. Park, W.Y. Kim, Y.H. Lee, S.H. Choi, et al., Carbon dioxide Fischer-Tropsch synthesis: A new path to carbon-neutral fuels, Appl Catal B Environ 202 (2017) 605–610, https://doi.org/10.1016/J.APCATB.2016.09.072.

[15] J. Wei, Q. Ge, R. Yao, Z. Wen, C. Fang, L. Guo, et al., Directly converting CO2 into a gasoline fuel, Nat. Commun. 8 (2017) 15174, https://doi.org/10.1038/ncomms15174.

[16] F. Jiang, B. Liu, S. Geng, Y. Xu, X. Liu, Hydrogenation of CO2 into hydrocarbons: Enhanced catalytic activity over Fe-based Fischer-Tropsch catalysts, Cat. Sci. Technol. 8 (2018) 4097–4107, https://doi.org/10.1039/c8cy00850g.

[17] Z. Shi, H. Yang, P. Gao, X. Chen, H. Liu, L. Zhong, et al., Effect of alkali metals on the performance of CoCu/TiO2 catalysts for CO2 hydrogenation to long-chain hydrocarbons, Chinese J Catal 39 (2018) 1294–1302, https://doi.org/10.1016/S1872-2067(18)63086-4.

[18] A.L. Tarasov, V.I. Isaeva, O.P. Tkachenko, V.V. Chernyshev, L.M. Kustov, Conversion of CO2 into liquid hydrocarbons in the presence of a Co-containing catalyst based on the microporous metal-organic framework MIL-53(Al), Fuel Process. Technol. 176 (2018) 101–106, https://doi.org/10.1016/j.fuproc.2018.03.016.

[19] J. Wei, R. Yao, Q. Ge, Z. Wen, X. Ji, C. Fang, et al., Catalytic Hydrogenation of CO2 to Isoparaffins over Fe-Based Multifunctional Catalysts, ACS Catal. 8 (2018) 9958–9967, https://doi.org/10.1021/acscatal.8b02267.

[20] S.M. Hwang, C. Zhang, S.J. Han, H.G. Park, Y.T. Kim, S. Yang, et al., Mesoporous carbon as an effective support for Fe catalyst for CO2 hydrogenation to liquid hydrocarbons, J. CO2 Util. 37 (2020) 65–73, https://doi.org/10.1016/J.JCOU.2019.11.025.

[21] Y. Wang, S. Kazumi, W. Gao, X. Gao, H. Li, X. Guo, et al., Direct conversion of CO2 to aromatics with high yield via a modified Fischer-Tropsch synthesis pathway, Appl Catal B Environ 269 (2020), 118792, https://doi.org/10.1016/J.APCATB.2020.118792.

[22] B. Yao, T. Xiao, O.A. Makgae, X. Jie, S. Gonzalez-Cortes, S. Guan, et al., Transforming carbon dioxide into jet fuel using an organic combustion-synthesized Fe-Mn-K catalyst, Nat. Commun. 11 (2020) 6395, https://doi.org/10.1038/s41467-020-20214-z.

[23] L. Guo, Y. Cui, P. Zhang, X. Peng, Y. Yoneyama, G. Yang, et al., Enhanced Liquid Fuel Production from CO2 Hydrogenation: Catalytic Performance of Bimetallic Catalysts over a Two-Stage Reactor System, ChemistrySelect 3 (2018) 13705–13711, https://doi.org/10.1002/slct.201803335.

[24] S. Saeidi, S. Najari, V. Hessel, K. Wilson, F.J. Keil, P. Concepción, et al., Recent advances in CO2 hydrogenation to value-added products — Current challenges and future directions, Prog. Energy Combust. Sci. 85 (2021), 100905, https://doi.org/10.1016/J.PECS.2021.100905.

[25] N. Meiri, R. Radus, M. Herskowitz, Simulation of novel process of CO2 conversion to liquid fuels, J CO2 17 (Util 2017,) 284–289, https://doi.org/10.1016/j.jcou.2016.12.008.

[26] S. Najari, G. Gróf, S. Saeidi, Enhancement of hydrogenation of CO2 to hydrocarbons via In-Situ water removal, Int. J. Hydrogen Energy 44 (2019) 24759–24781, https://doi.org/10.1016/j.ijhydene.2019.07.159.

[27] A.D.N. Kamkeng, M. Wang, J. Hu, W. Du, F. Qian, Transformation technologies for CO2 utilisation: Current status, challenges and future prospects, Chem. Eng. J. 409 (2021), 128138, https://doi.org/10.1016/j.cej.2020.128138.

[28] W.L. Becker, R.J. Braun, M. Penev, M. Melaina, Production of Fischer-Tropsch liquid fuels from high temperature solid oxide co-electrolysis units, Energy 47 (2012) 99–115, https://doi.org/10.1016/J.ENERGY.2012.08.047.

[29] M. Hillestad, Modeling the Fischer-Tropsch Product Distribution and Model Implementation, Chem. Prod. Process Model. 10 (2015) 147–159, https://doi.org/10.1515/cppm-2014-0031.

[30] N. Meiri, Y. Dinburg, M. Amoyal, V. Koukouliev, R.V. Nehemya, M.V. Landau, et al., Novel process and catalytic materials for converting CO2 and H2 containing mixtures to liquid fuels and chemicals, Faraday Discuss. 183 (2015) 197–215, https://doi.org/10.1039/c5fd00039d.

[31] T.J. Donnelly, I.C. Yates, C.N. Satterfield, Analysis and Prediction of Product Distributions of the Fischer-Tropsch Synthesis, Energy Fuel 2 (1988) 734–739, https://doi.org/10.1021/ef00012a003.

[32] D. Selvatico, A. Lanzini, M. Santarelli, Low Temperature Fischer-Tropsch fuels from syngas: Kinetic modeling and process simulation of different plant configurations, Fuel 186 (2016) 544–560, https://doi.org/10.1016/j.fuel.2016.08.093.

[33] B. Todic, T. Bhatelia, G.F. Froment, W. Ma, G. Jacobs, B.H. Davis, et al., Kinetic model of Fischer-Tropsch synthesis in a slurry reactor on Co-Re/Al2O3 catalyst, Ind. Eng. Chem. Res. 52 (2013) 669–679, https://doi.org/10.1021/ie3028312.

[34] J.P. Stempien, M. Ni, Q. Sun, S.H. Chan, Thermodynamic analysis of combined Solid Oxide Electrolyzer and Fischer-Tropsch processes, Energy 81 (2015) 682–690, https://doi.org/10.1016/J.ENERGY.2015.01.013.

[35] G. Cinti, A. Baldinelli, A. Di Michele, U. Desideri, Integration of Solid Oxide Electrolyzer and Fischer-Tropsch: A sustainable pathway for synthetic fuel, Appl. Energy 162 (2016) 308–320, https://doi.org/10.1016/J.APENERGY.2015.10.053.

[36] Stratas Advisors. Phase-out of RON 80 Gasoline Progresses in the CIS. 2021.

[37] M.V. Landau, R. Vidruk, M. Herskowitz, Sustainable production of green feed from carbon dioxide and hydrogen, ChemSusChem 7 (2014) 785–794, https://doi.org/10.1002/cssc.201301181.

[38] R.G. Grim, Z. Huang, M.T. Guarnieri, J.R. Ferrell, L. Tao, J.A. Schaidle, Transforming the carbon economy: challenges and opportunities in the convergence of low-cost electricity and reductive CO2 utilization, Energ. Environ. Sci. (2020) 472–494, https://doi.org/10.1039/c9ee02410g.